# Expanded View Figures

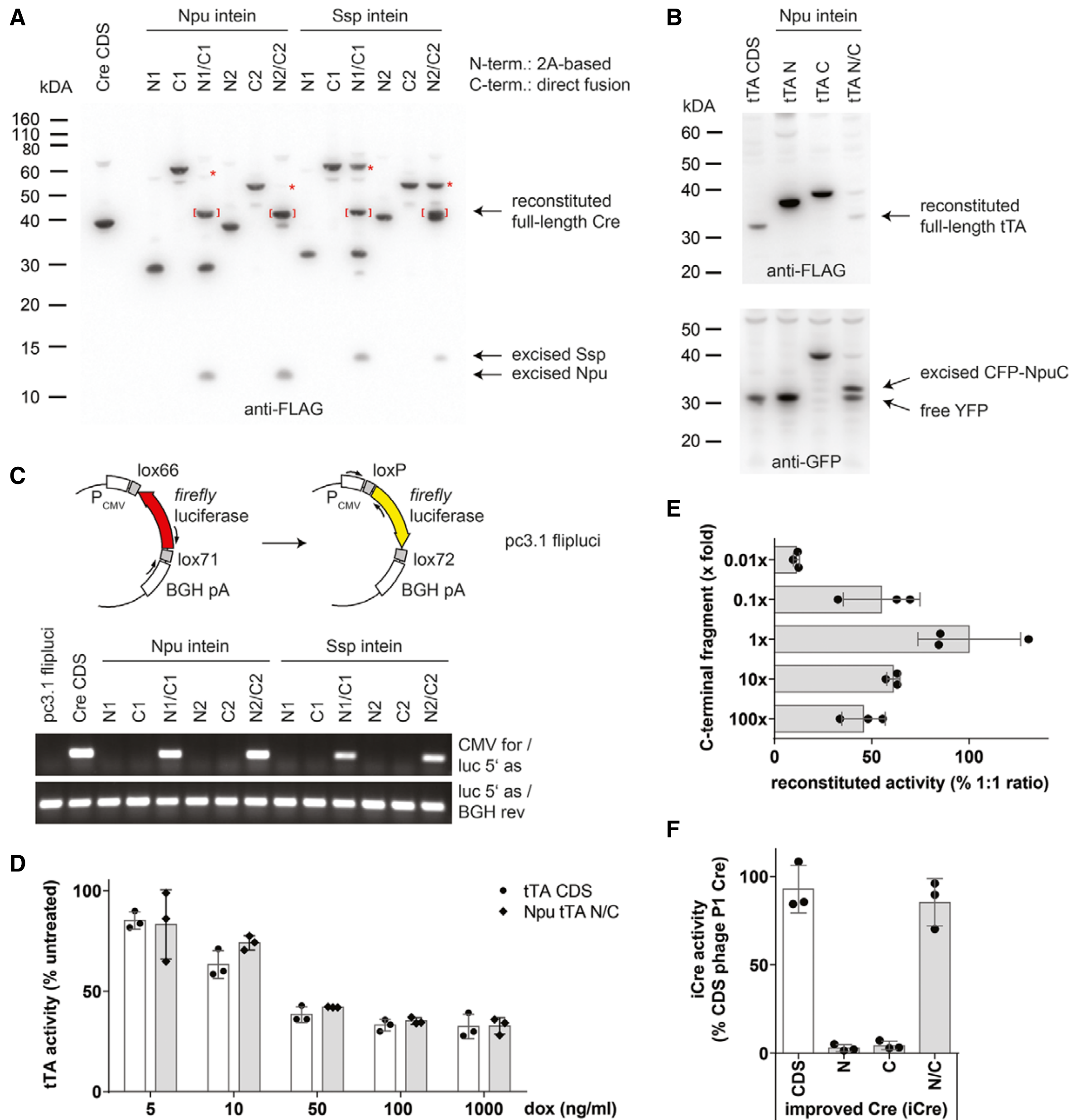


**Figure EV1.** ***In vitro*** **characterization of split-effector molecules.**

A Western blot analysis of Cre reconstitution by intein-mediated *trans*-splicing. Brackets indicate reconstituted full-length Cre protein, and asterisks denote near complete conversion of C-terminal effector fragment using *Npu*-based split-Cre pairs.

B Reconstitution of full-length tTA protein by intein-mediated *trans*-splicing.

C PCR-based analysis of Cre-mediated DNA recombination.

D Quantification of tTA activity by dual luciferase assays in the presence of doxycycline (dox). Data depicted as mean ± SD, $n = 3$.

E Reconstitution of biologically active tTA protein at different ratios of N- and C-terminal fragments. A constant amount of *Npu* tTA N was co-transfected with varying amounts of *Npu* tTA C to mimic potential differences in expression levels. tTA activity was quantified by dual luciferase assays. Data depicted as mean ± SD, $n = 3$.

F *In vitro* testing of split-iCre reconstitution used for insertion into endogenous *Ccsp* and *Spc* gene loci. Phage P1-derived Cre fragments within the *Npu* N1/C1 split-pair were replaced by equivalent sequences from a codon-improved Cre recombinase (iCre). Cre activity was quantified by dual luciferase assays. Data depicted as mean ± SD, $n = 3$.

Data information: Npu, *Nostoc punctiforme*; Ssp, *Synechocystis sp.*; CDS, coding sequence.

Source data are available online for this figure.

© 2019 The Authors 

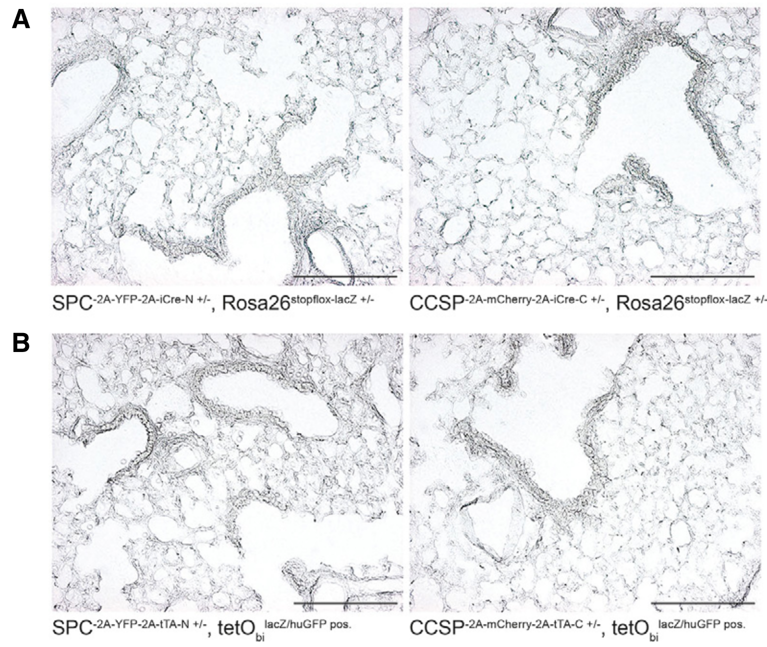


**Figure EV2. Individual split-effector halves are functionally inactive.**

A, B β-galactosidase staining of lung sections from N- and C-terminal. (A) split-Cre or (B) split-tTA knock-in strains combined with corresponding reporter alleles as indicated. Scale bar: 200 μm.

 © 2019 The Authors

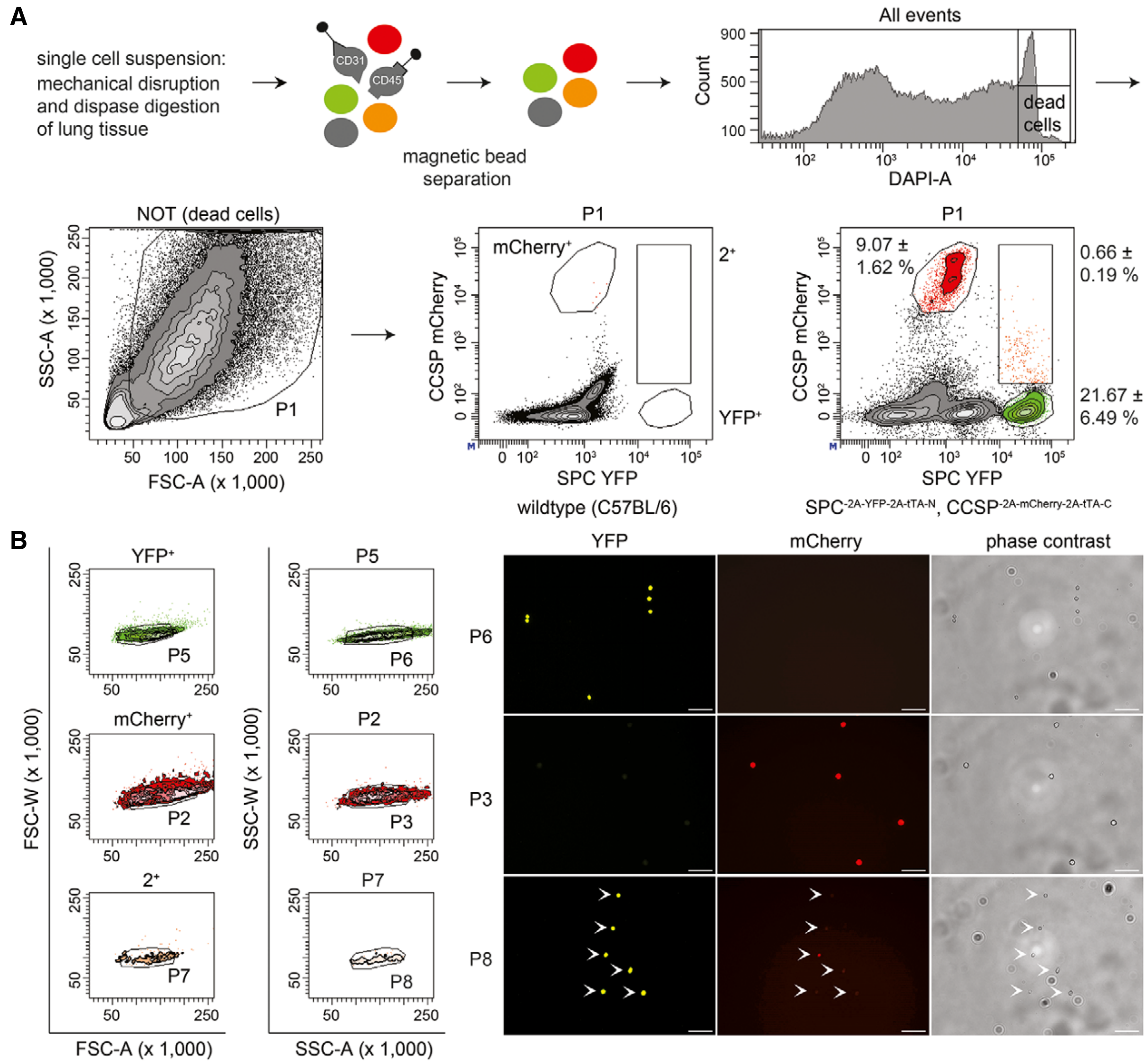


**Figure EV3. Isolation of AT2 cells, Club cells, and BASCs by FACS.**

A Hematopoietic and endothelial cells were separated from lung cell suspensions using magnetic beads (anti-CD45 and anti-CD31). Viable epithelial cells were analyzed for mCherry and YFP fluorescence to establish the gates for mCherry$^+$ (Club cells), YFP$^+$ (AT2 cells), and 2$^+$ (BASCs). Cell abundance is shown as percentage of total P1 cells. Data depicted as mean ± SD, $n$ = 10.

B Doublet exclusion based on forward (FSC) and side scatter (SSC) width versus amplitude plots and subsequent fluorescence microscopy of FACS-isolated single cells. Scale bar: 50 µm.

Source data are available online for this figure.

© 2019 The Authors

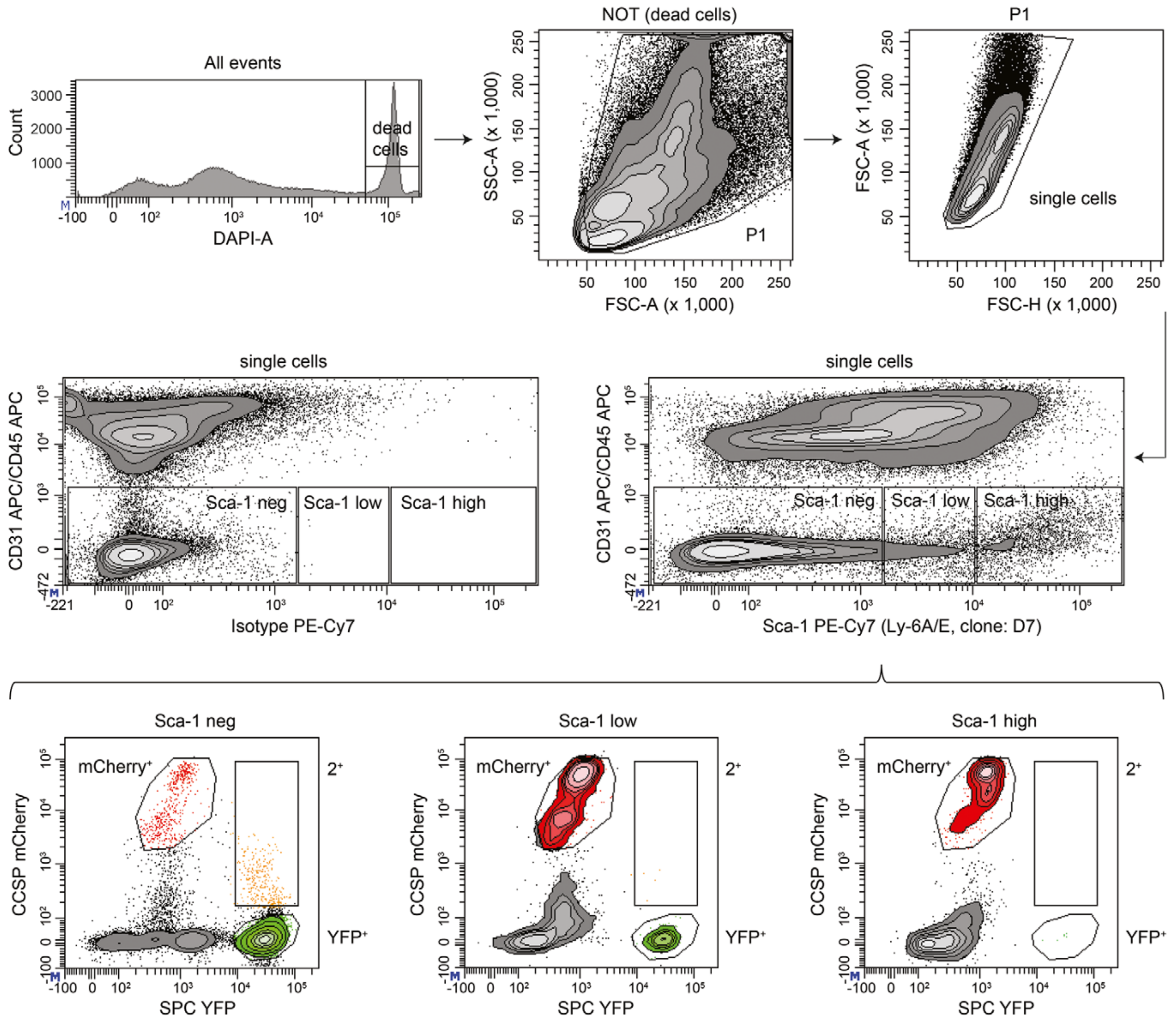


**Figure EV4. Flow cytometric analysis of stem cell antigen-1 (Sca-1) expression.**

Viable single cells of non-endothelial and non-hematopoietic origin (CD31/CD45 neg) derived from lungs of BASC viewer mice were analyzed for Sca-1 immunoreactivity to establish the gates Sca-1 neg/low/high. Sca-1 fractions were subsequently analyzed for mCherry and YFP fluorescence to identify Club cells (mCherry$^+$), AT2 cells (YFP$^+$), and BASCs (2$^+$).

 © 2019 The Authors

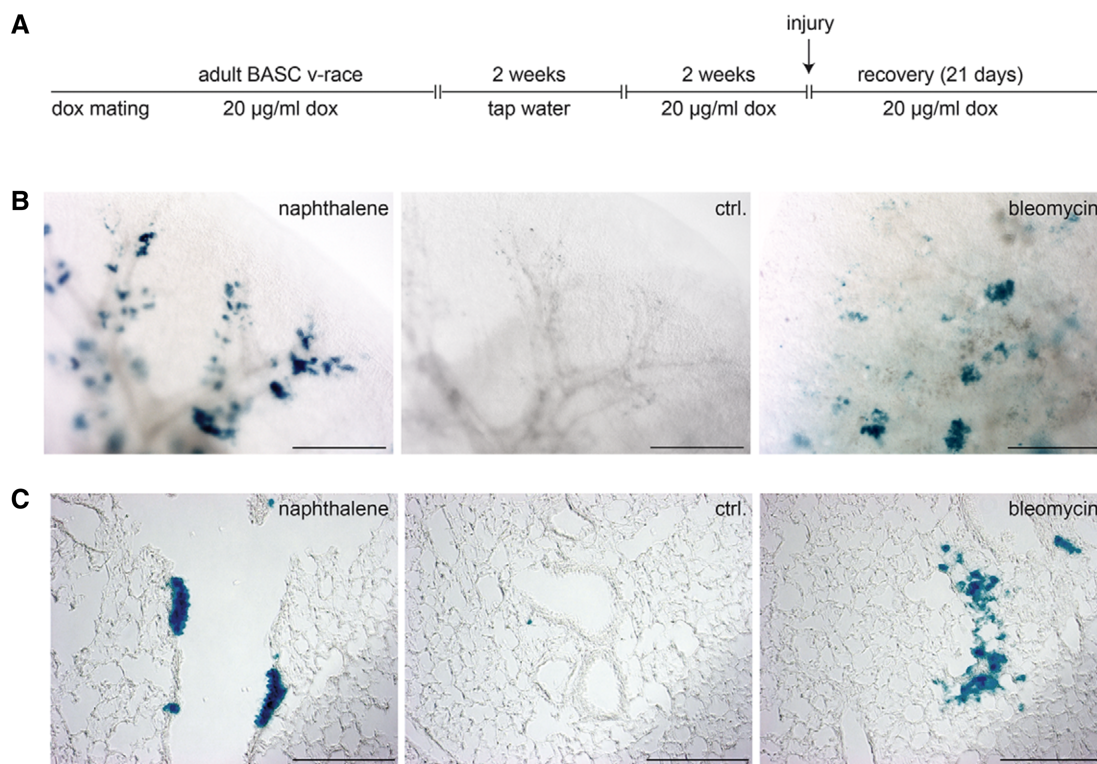


**Figure EV5. Clonal analysis of BASCs forming clusters of bronchiolar and alveolar epithelial cells.**

A Schematic outline of the treatment regimen. BASC v-race animals were already treated with doxycycline during breeding. Doxycycline treatment of offspring was continued until adulthood. To induce labeling of single BASCs, doxycycline treatment was temporarily suspended for 2 weeks when mice reached an age of 2 months. Two weeks after re-initiation of doxycycline treatment, lung injury was induced by administration of naphthalene or bleomycin.

B, C β-galactosidase staining of cleared whole lung preparations (scale bar: 1 mm) and lung sections (scale bar: 200 µm) from control and injured BASC v-race animals 21 days after injury. Labeling of single BASCs resulted in distinct clusters of β-gal$^+$ cells in the bronchiolar (Club cells) and alveolar (AT2 cells) compartment.